Toxicity of *Melaleuca alternifolia* essential oil to the mitochondrion and NAD$^+$/NADH dehydrogenase in *Tribolium confusum*

Min Liao [1, 2] , **Qian-Qian Yang** [1] , **Jin-Jing Xiao** [1] , **Yong Huang** [1] , **Li-Jun Zhou** [1] , **Ri-Mao Hua** [2] , **Hai-Qun Cao** Corresp. [1, 2]

[1] School of Plant Protection, Anhui Agricultural University, Hefei, China

[2] Provincial Key Laboratory for Agri-Food Safety, Anhui Province, Anhui Agricultural University, Hefei, China

Corresponding Author: Hai-Qun Cao
Email address: haiquncao@163.com

Background. In our previous study, *Melaleuca alternifolia* essential oil (EO) was considered to have an insecticidal effect by acting on the mitochondrial respiratory chain in insects. However, the mode of action is not fully understood.

Methods. In this study, we investigated the insecticidal efficacy of the *M. alternifolia* EO against another major stored-product pest, *Tribolium confusum* Jacquelin du Val. Rarefaction and vacuolization of the mitochondrial matrix were evident in oil-fumigated *T. confusum* adults. **Results.** Alterations to the mitochondria confirmed the insecticidal effect of the *M. alternifolia* EO. Furthermore, comparative transcriptome analysis of *T. confusum* using RNA-seq indicated that most of the differentially expressed genes were involved in insecticide detoxification and mitochondrial function. The biochemical analysis showed that the intracellular NAD$^+$/NADH ratio is involved in the differential effect of the *M. alternifolia* EO.

Discussion. These results led us to conclude that NAD$^+$/NADH dehydrogenase may be the prime target site for the *M. alternifolia* EO in insects, leading to blocking of the mitochondrial respiratory chain.

Toxicity of *Melaleuca alternifolia* essential oil to the mitochondrion and NAD^+/NADH dehydrogenase in *Tribolium confusum*

Min Liao[1, 2†], Qian-Qian Yang[1†], Jin-Jing Xiao[1], Yong Huang[1], Li-Jun Zhou[1], Ri-Mao Hua[2], Hai-Qun Cao[1, 2*]

[1] School of Plant Protection, Anhui Agricultural University, Hefei, Anhui Province 230036, China;

[2] Provincial Key Laboratory for Agri-Food Safety, Anhui Province 230036, China.

† These authors contributed equally to this work.

* Corresponding author: Hai-Qun Cao

E-Mails: haiquncao@163.com (H.-Q.C.).

16 **Abstract**

17 **Background.** In our previous study, *Melaleuca alternifolia* essential oil (EO) was considered to
18 have an insecticidal effect by acting on the mitochondrial respiratory chain in insects. However,
19 the mode of action is not fully understood.

20 **Methods.** In this study, we investigated the insecticidal efficacy of the *M. alternifolia* EO against
21 another major stored-product pest, *Tribolium confusum* Jacquelin du Val. Rarefaction and
22 vacuolization of the mitochondrial matrix were evident in oil-fumigated *T. confusum* adults.

23 **Results.** Alterations to the mitochondria confirmed the insecticidal effect of the *M. alternifolia*
24 EO. Furthermore, comparative transcriptome analysis of *T. confusum* using RNA-seq indicated
25 that most of the differentially expressed genes were involved in insecticide detoxification and
26 mitochondrial function. The biochemical analysis showed that the intracellular NAD^+/NADH ratio
27 is involved in the differential effect of the *M. alternifolia* EO.

28 **Discussion.** These results led us to conclude that NAD^+/NADH dehydrogenase may be the prime
29 target site for the *M. alternifolia* EO in insects, leading to blocking of the mitochondrial respiratory
30 chain.

31

INTRODUCTION

Essential oils (EOs) obtained from aromatic plants by steam distillation are regarded as a new and safe alternative to conventional insecticides because of their bioactive potential and high volatility (Bai et al. 2015; Liang et al. 2016). The volatile nature of plant essential oils reduces concerns regarding residues of their constituents on stored grains, which mitigates environmental contamination and effects on non-target organisms (Li et al. 2013; Polatoglu et al. 2016). The potential for synergistic or additive effects between the volatile secondary metabolites of essential oils, which act on insects via various targets and mechanisms, is also an advantage (Abdelgaleil et al. 2015).

EOs are mixtures of volatile secondary metabolites, mainly monoterpenes and sesquiterpenes; therefore, they have various modes of action in insects. It is difficult to separate and purify an active substance to study its mechanisms. Moreover, the insecticidal activity of an essential oil can be attributed to the synergistic effects of its major components (Wu et al. 2015); therefore, all the major components need to be considered while assessing the mechanism of an essential oil. The mechanisms underlying the toxicity of EOs have been explored for decades. To date, most of the studies focused on enzyme inhibition or induction (Ali-Shtayeh et al. 2018; Kiran et al. 2017; Vanhaelen et al. 2001). The main targets of EOs are neurotoxic target enzymes such as acetylcholinesterase and a variety of detoxifying enzymes such as glutathione *S*-transferase (GST) and carboxylesterase (CarE) (Oter et al. 2018). EOs have lethal and sublethal effects on pests that attack stored grains, and they are frequently applied via fumigation by stored-grain managers (Haddi et al. 2015; Silva et al. 2017). Thus, the activity of essential oils may cause

53 abnormal respiration (de Carvalho et al. 2017), which is similar to the effect of octopamine (Enan
54 2005); however, relatively little is known about the underlying mechanisms, particularly the
55 mitochondrial electron transport chain.

56 Recently, transcriptome profiling analysis has increased our understanding of insect response
57 to various stressors (Chen et al. 2016; Du et al. 2016). RNA-seq is an effective tool for studying
58 the extensive regulation at transcriptional levels (Clements et al. 2016; Hamisch et al. 2012), and
59 it can be used for characterizing the complexity of mitochondrial transcriptomes (Stone &
60 Storchova 2015). In our previous study, we had reported, for the first time, a comprehensive
61 transcriptome analysis of the maize weevil, *Sitophilus zeamais*, to identify the genes and pathways
62 that are likely to be changed upon exposure to the essential oil obtained from *Melaleuca*
63 *alternifolia* (Liao et al. 2016). Our findings suggested that the mitochondrial electron transport
64 chain is a likely target in insects. Such information contributes to new insights on the biological
65 response of insects to EOs and helps us in understanding the molecular mechanisms underlying
66 the insecticidal activity of plant EOs.

67 *M. alternifolia* is derived from an Australian plant, *Melaleuca leucadendron*, and it was
68 developed to meet increasing demands for its monoterpene-rich EOs (Bustos-Segura et al. 2015).
69 Notably, the major component, terpinen-4-ol, showed distinct fumigant toxicity against the pests
70 of stored grains: 6.78 mg/L air of median lethal concentration (LC_{50}) for *S. zeamais* (Liao et al.
71 2016). Terpinen-4-ol has also been found in the most EOs reported in previous studies and should
72 be studied further (Abdelgaleil et al. 2015; Brahmi et al. 2016; Yeom et al. 2013).

73 To obtain information on the fumigant toxicity of *M. alternifolia* EO and its chemical

compounds against stored grain insects and identify a better chemotype, we studied the toxicity of *M. alternifolia* EO against the confused flour beetle (*Tribolium confusum* Jacquelin du Val.), which is closely related to the flour beetle *Tribolium castaneum* (Herbst) (Golestan et al. 2015). To expand on the applicability of our previous transcriptomic analysis and provide a clearer picture of the mode of action of natural insecticides, we also performed RNA-seq analysis of the *T. confusum* transcriptome to investigate changes in the abundance of mitochondrial transcripts after exposure to the *M. alternifolia* EO. To verify the reliability of the RNA-seq data, we tested the inhibitory effects of the EO on NAD^+/NADH dehydrogenase, which is a possible insecticidal target. Subsequently, we assessed the action of the *M. alternifolia* EO in degrading the mitochondria in the cells obtained from oil-fumigated *T. confusum.* To our knowledge, no studies on the molecular events underlying the response of *T. confusum* to plant EOs have been performed or published.

MATERIALS AND METHODS

EO and chemicals

The EO (density, 0.8978) was purchased from Fujian Senmeida Biological Technology Co., Ltd (China). Terpinen-4-ol (40.09%), γ-terpinene (21.85%), α-terpinene (11.34%), α-terpineol (6.91%), and 1,8-cineole (1.83%) were the major compounds.

Insect culture

A culture of *T. confusum* was maintained in the laboratory, and the insects were not exposed to any insecticides. For insect culture, the larvae were reared on sterilized whole wheat at 28 ± 1 °C and 68 ± 5 °C relative humidity under complete darkness. Then, pupae of the same age were

95 collected and transferred to a new container. After emergence, the adults were reared to about 2
96 weeks of age for use in the subsequent experiments.

97 **Fumigant toxicity assay**

98 The fumigant toxicity of *M. alternifolia* EO against *T. confusum* was determined according to our
99 previous protocol (Liao et al. 2016). For oil exposure, 30 adults were exposed to serial dilution
100 doses in sealed gas-tight 300-mL glass jars and incubated for 24, 48, and 72 h at 28 °C. Drops of
101 the oil (1.8, 2.1, 2.5, 3.2, and 4.0 mL) were applied with an Automatic Micro-applicator (Burkard
102 900- X; Burkard Scientific Co., Ltd, USA) to a piece of filter paper (2 × 3 cm), and the filter paper
103 was attached to the undersurface of the jar lid. Equivalent groups of control adults were treated
104 similarly, but without exposure to the oil. Three biological replicates were maintained for each
105 treatment. For the EO constituents, the protocol for fumigant toxicity was determined using the
106 above-mentioned process, and serial dilutions were prepared and applied to filter paper. In
107 addition, *T. confusum* specimens exposed to LC_{50} (6.37 mg/L air) of oil for 12, 24, 36, 48, 60, and
108 72 h were collected and washed twice or three times with pre-cooled saline, flash-frozen in liquid
109 nitrogen, and stored at -80 °C for the subsequent bioassays.

110 **Transmission electron microscopy of mitochondria**

111 Cells were obtained from the thorax for transmission electron microscopy (TEM) by dissecting
112 the insects at 24, 48, and 72 h after the oil treatment. The samples were fixed in a mixture of 5%
113 glutaraldehyde and 0.1 M sodium cacodylate (pH 7.2) for 24 h. After fixation, the samples were
114 washed, dehydrated, and embedded in pure resin, according to the protocol of Correa et al. (2014).
115 After polymerization in gelatin capsules, ultrathin sections were placed on copper grids and

116 subsequently observed and photographed using a transmission electron microscope (HT7700;
117 Hitachi, Japan).

118 **RNA sequencing**

119 Total RNA was extracted from oil treatment and control groups (collected at 24 h) with TRIzol
120 reagent (Kangwei Century Biological Co., Ltd., China), according to the manufacturer's
121 instructions, and treated with DNase I (Sangon Biotech, Shanghai, China). The RNA quality was
122 checked with a 2100 Bioanalyzer (Agilent Technologies, USA). Library construction and Illumina
123 sequencing were performed at BGI-Tech (Wuhan, China). For cDNA library construction, 5 μg of
124 RNA per sample from three biological replicates were combined and used. Two cDNA libraries
125 were constructed for the oil treatment and control groups. For Illumina sequencing, which followed
126 the protocol of the Illumina TruSeq RNA Sample Preparation Kit (BGI-Tech, Wuhan, China), 2 ×
127 100-bp paired-end reads were sequenced using Illumina HiSeq™ 4000 (Illumina Inc., USA), with
128 the depth of 6 G for each sample. The reads were submitted to the NCBI Sequence Read Archive
129 (SRA; accession number, SUB2742979).

130 **Bioinformatic analyses**

131 The reads for the treatment and control groups were mapped to the 165.944-Mb *T. castaneum*
132 reference genome obtained from NCBI (BioProjects: PRJNA12540) by using TopHat v.2.08 (Kim
133 et al. 2013a), with quality aware alignment algorithms (Bowtie v.2.2.5) (Langmead et al. 2009).

134 The raw RNA-seq reads were assessed for quality with FastQC (version 0.11.4; Babraham
135 Bioinformatics, Cambridge, UK) and saved as FASTQ files with default parameters (Cock et al.
136 2010). Then, *de novo* assembly of the clean reads was performed using the Trinity method (version

2.0.6) (Grabherr et al. 2011). All the unique Trinity contigs were analyzed using BlastX (E-value $< 10^{-5}$) against the protein databases Nr (Agarwala et al. 2016), Nt (Agarwala et al. 2016), COG (Tatusov et al. 2000), KEGG (Kanehisa & Goto 2000), Swiss-Prot, and InterPro using InterProScan5 with default parameters. To annotate the assembled sequences with GO terms, Nr Blast results were imported into Blast2GO (Conesa et al. 2005).

Transcript abundance was calculated as fragments per kilobase of transcript per million fragments mapped (FPKM) for each sample (Li & Dewey 2011). Differential gene expression analysis (fold changes) and related statistical significance in pair-wise comparison were performed using the DESeq program (http://www-huber.embl.de/users/anders/DESeq/) (Anders & Huber 2010). The DEGs were identified using a false discovery rate (FDR) threshold ≤ 0.001 and absolute value of log2Ratio ≥ 1 (Hao et al. 2016). Genes with an adjusted P-value were used for controlling FDR, and those with a threshold < 0.05 were classified as differentially expressed (Ma et al. 2015).

For each DEG, GO and KEGG enrichment analyses were conducted using the DESeq R package (http://www.geneontology.org/ and http://www.genome.jp/kegg/, respectively). The GOslim annotations results were then classified into three main classes: molecular function, biological process, and cellular component. The KEGG database was used to identify significantly enriched metabolic pathways or signal transduction pathways.

Quantitative real-time PCR

qRT-PCR was used to further validate and quantify the RNA levels for 20 selected genes that encode NADH or NAD^+ by using the iCycler iQ Real-time Detection System (Bio-Rad, Hercules, CA, USA). Gene-specific primers were designed using Primer Premier 5, and the sequences are

158 listed in Table S1. The house-keeping gene glyceraldehyde 3-phosphate dehydrogenase (GAPDH)
159 was used as the reference gene, as proposed by Prentice et al (Pan et al. 2015). For the qRT-PCR
160 analysis, cDNA templates were diluted 20-fold in nuclease-free water. Then, mRNA levels were
161 measured in triplicate (technical repeats) with qPCR by using the SYBR Green Master Mix
162 (Vazyme Biotech Co., Ltd, Nanjing, China), according to the manufacturer's instructions. PCR
163 amplification was performed in a total volume of 20.0 μL containing 10.0 μL of the SYBR Master
164 Mix, 0.4 μL of each primer (10 μM), 2.0 μL of cDNA, and 7.2 μL of RNase-free water. The
165 amplification procedure was composed of an initial denaturation step at 95 °C for 5 min, followed
166 by 40 cycles of 95 °C for 10 s and 60 °C for 30 s and the melting curve step at 95 °C for 15 s, 60
167 °C for 60 s, and 95 °C for 15 s. Gene expression was quantified (mean ± SD) as relative fold
168 change by using the $2^{-\Delta\Delta CT}$ method (Schmittgen & Livak 2008).

169 **Measurement of intracellular NAD^+/NADH ratio**

170 Both oxidized and reduced forms of intracellular NAD were determined using an NAD(H)
171 quantification kit (Nanjing Jiancheng Bioengineering Institute, Nanjing, China). Briefly, 0.1 g of
172 the test insects were collected at 12, 24, 36, 48, 60, and 72 h and extracted with 1 mL of
173 NAD^+/NADH extraction buffer in three freeze/thaw cycles. The samples were centrifuged at
174 10000 × *g* for 5 min at 4 °C. Then, 0.5 mL of the extracted NADH or NAD^+ supernatant was
175 transferred to a centrifuge tube and neutralized with an equal volume of the opposite extraction
176 buffer. The samples were centrifuged at 10000 × *g* for 10 min at 4 °C and then used for the
177 subsequent bioassays. NADH or NAD^+ cycling mix was prepared according to the manufacturer's
178 protocol (Nanjing Jiancheng Bioengineering Institute, Nanjing, China). Finally, absorbance was

179 measured at 570 nm. In addition, the concentration of the total protein was determined using the
180 total protein quantitative assay (Nanjing Jiancheng Bioengineering Institute, Nanjing, China).
181 Three replicates were used for each treatment, and each replicate was determined three times.

182 **Statistical analysis**

183 The mortality rates observed in the toxicity bioassays were corrected for the control group by using
184 Abbott's formula (Abbott 1925). All data are expressed as mean ± SE values of three independent
185 experiments and analyzed using one-way nested analysis of variance and unpaired sample *t*-test.
186 A significant difference was accepted at a p value < 0.05. An extremely significant difference was
187 accepted at p value < 0.01. The LC_{50} values were evaluated using probit analysis (Hubert & Carter
188 1990), and corresponding confidence intervals at 95% probability were obtained using IBM SPSS
189 Statistics 22.0 (SPSS, USA). Figures depicting the effects of the EO on enzymatic activities and
190 the qRT-PCR results were created using Origin Pro 9.0 (Origin Lab Corporation, USA).

191 **RESULTS**

192 **Fumigant toxicity of *M. alternifolia* EO and constituents**

193 To investigate the toxicity of the *M. alternifolia* EO against *T. confusum* adults, we performed the
194 fumigation assay. The results show that *M. alternifolia* EO has potent fumigant toxicity (Fig. 1a),
195 and the effect of fumigation gradually increased over time (24 h, 48 h, and 72 h); the corresponding
196 LC_{50} values were 7.45, 7.09, and 6.37 mg/L air, respectively (Fig. 1b). The largest dose of 11.97
197 mg/L air EO caused 91.11%, 97.78%, and 98.86% mortality, respectively, in the *T. confusum*
198 adults.

199 In particular, terpinen-4-ol was the most potent toxicant with an LC_{50} value of 3.83 mg/L air

(Fig. 1c). In the *M. alternifolia* EO, terpinen-4-ol was the main component (40.09% of the EO), indicating that terpinen-4-ol is the major contributor to the fumigant toxicity of the EO. In addition, γ-terpinene and α-terpinene exhibited weaker fumigant toxicity (LC_{50} = 28.52 and 44.53 mg/L air, respectively) against *T. confusum*.

TEM of mitochondria

An ultra-structural examination of the morphology of the mitochondria from untreated and oil-fumigated *T. confusum* larvae is shown in Fig. 2. In the untreated *T. confusum* larvae, the mitochondria have highly electron-dense cristae, membranes, and matrix (Fig. 2a, c, e). However, the mitochondria in the columnar and regenerative nidi cells from the thorax of the oil-treated *T. confusum* larvae had undergone ultra-structural changes detected by the vacuolization of the mitochondrial matrix (Fig. 2b, d, f), when compared with the non-fumigated adults. The vacuolization increased with time after the oil treatment and, in severe cases, caused fragmentation of the mitochondria.

Illumina sequencing and *de novo* assembly

To obtain a global, comprehensive overview of the *T. confusum* transcriptome, RNA was extracted from the treatments and control groups. A total of 126,280,032 paired-end reads (100 bp) were generated from the samples by using the Illumina HiSeq™ 4000 platform. Then, 89,342,546 clean reads were obtained by preprocessing and filtering the reads (low-quality sequences were removed; Table 1). Subsequently, the clean reads were subjected to transcriptome assembly by using the Trinity software package (Grabherr et al. 2011), and 28,885 assembled unigenes were generated using overlapping information from high-quality reads, which accounted for 36,998,010

221 bp (Table 1). Of the assembled unigenes, approximately 38.54% were ≤600 bp and 61.46% were
222 >500 bp. The average length of the unigenes was 1,280 bp, with an N50 length of 2,097 bp and
223 mean length of 1280 bp. The length distribution of the unigenes is shown in Fig. 3a.

224 **Functional annotation of *T. confusum* transcripts**

225 All the assembled unigenes were aligned against seven public databases (Table 1). Of the 28,885
226 assembled unigenes, 23,160 (80.18%) exhibited sequence similarity to a sequence within the Nr
227 database; 23,571 (81.60%) unigenes were annotated in at least one database, indicating that just a
228 few unigenes (18.40%) could not be identified. The homologous genes that showed the best match
229 (54.24%) were from *T. castaneum* (91.82%). On the basis of the Nr annotation, GO functional
230 analysis of the unigenes was performed. A total of 6,333 (21.92%) unigenes were assigned to the
231 biological process, molecular function, and cellular component categories, including 57 GO terms
232 (Fig. 3b). In addition, 18,074 (62.57%) unigenes were divided into 42 subcategories and 295
233 KEGG pathways by using the KEGG annotation system with default parameters to predict the
234 metabolic pathways (Fig. 3c).

235 **Differential expression analysis and pathway enrichment**

236 The sequence analysis and annotation of all the unigenes in *S. zeamais* fumigated by the *M.*
237 *alternifolia* EO provided some valuable information for analyzing the *T. confusum* transcriptome.
238 From the 23,571 unigenes identified in the analysis, we chose to focus on transcripts encoded by
239 the genes associated with known mechanisms to cope with xenobiotic compounds, including
240 quantitative or qualitative changes in major detoxification enzymes and transporters to decrease
241 exposure (pharmacokinetic mechanisms) or changes in target site sensitivity (pharmacodynamic

242 mechanisms) (Bajda et al. 2015). Specifically, changes in the expression levels of four classes of
243 enzymes and proteins (GST, CarE, cytochrome P450 monooxygenases, and mitochondrial
244 respiratory chain-related proteins) were investigated to determine whether patterns emerged in the
245 upregulation or downregulation of specific transcripts. The transcriptome of *T. confusum* showed
246 that the largest and most abundant group was ATPase transporters, followed by cytochrome P450s;
247 some of them may be involved in insecticidal mechanisms. The transcriptome also showed five
248 possible NAD^+/NADH dehydrogenase transcripts, which may be the main targets for the EO.

249 For comparison, FPKM of each transcript was calculated to estimate the expression levels
250 between the oil-fumigated and oil-free samples. The important DEGs (999 upregulated and 1,209
251 downregulated) were identified on the basis of threshold FDR < 0.01 and fold change 2 between
252 the oil-fumigated and oil-free samples. To annotate these DEGs, both GO and KEGG functional
253 analyses were performed.

254 The GO annotation analysis classified 632 DEGs into three GO categories and 339 terms
255 (Fig. S1a). In the molecular function category, 560 DEGs were classified into 11 terms, namely,
256 antioxidant activity, binding, catalytic activity, electron carrier activity, enzyme regulator activity,
257 guanyl-nucleotide exchange factor activity, molecular transducer activity, nucleic acid binding
258 transcription factor activity, receptor activity, structural molecule activity, and transporter activity.

259 Among the DEGs, 1,180 unigenes were mapped to 287 different KEGG pathways and five
260 categories (Fig. S1b). According to the threshold of Q value < 0.05, 22 pathways were significantly
261 enriched (Table S2). Many DEGs were significantly enriched in the metabolism pathways
262 associated with respiration and metabolism of xenobiotics, suggesting that abnormal respiration

and metabolic disorders occurred in the *T. confusum* adults after fumigation with the *M. alternifolia* EO. In addition, 92 possible insect hormone biosynthesis transcripts, some of which are known targets of chlorbenzuron, were detected (Xu et al. 2017).

To verify the expression patterns of the DEGs involved in metabolism, 20 genes were selected for qRT-PCR analysis. As shown in Fig. 4, similar trends of upregulation/downregulation of the selected DEGs were observed between the qRT-PCR and transcriptome data, confirming the accuracy of our transcriptome profiling.

NAD^+/NADH ratio in *T. confusum* fumigated with the *M. alternifolia* EO

On the basis of a previous study on *S. zeamais* and the above-mentioned results, the NAD^+/NADH ratio in *T. confusum* fumigated with the *M. alternifolia* EO was measured to investigate whether the EO acts on NAD^+/NADH. In the non-fumigated insects, a decrease in NAD^+ and NADH levels was observed over the course of 24–48/60 h, which may be affected by starvation. Further, we found that treatment with 6.37 mg/L EO significantly increased NAD^+ (Fig. 5a) but decreased NADH (Fig. 5b) levels at 12–48 h, when compared with the non-fumigated samples; however, the opposite trend was observed after 60 h. The ratio of NAD^+/NADH in *T. confusum* from 12 to 60 h after treatment decreased (significantly in 24–48 h) and increased after 60 h, but not effectively (Fig. 5c).

DISCUSSION

In this study, similar toxicity patterns were observed for the *M. alternifolia* EO and major compounds (Liao et al. 2016), which confirms this EO as a possible alternative to the natural fumigants currently in use. α-terpinene and γ-terpinene possessed weaker fumigant toxicity against

284 *T. confusum* than terpinen-4-ol and α-terpineol, showing that the oxygen-containing compounds
285 could cause a remarkable change in bioactivity. Kim et al. (2013b) described a similar structure–
286 activity relationship among oil constituents with aldehyde, ketone, and alcohol groups and
287 hydrocarbons against rice weevil adults. Terpinen-4-ol and α-terpineol have similar fumigant
288 toxicity, which was more toxic than the EO. The two constituents accounted for 46% of the EO
289 content, and about 2-fold LC_{50} of *M. alternifolia* EO. Thus, the fumigant toxicity of the *M.*
290 *alternifolia* EO may be attributable to a synergistic effect of the activities of the oil constituents.
291 We deduced that the terpinen-4-ol chemotype is the main insecticidal active component, which
292 accounted for 40% of the EO content. The amount of terpinen-4-ol directly affects the insecticidal
293 activity of the EO, according to the fumigant toxicities of the constituents of the EO. Terpinen-4-
294 ol is also found in many reported EOs (Du et al. 2014; Liang et al. 2017). Thus, we suggest that
295 the chemotypes of oils rich in terpinen-4-ol should be explored as potential natural insecticides.
296 EOs have produced remarkable results; however, several barriers stand in the way of their
297 application in agriculture. Their unclear mode of action is one of the most significant barriers. An
298 EO is a well-known mixture of volatile secondary metabolites that operate via several modes of
299 action. In insects, octopamine (Enan 2005) and GABA receptor (Enan 2001) are considered targets
300 for EO activity. In our previous study, the *M. alternifolia* EO was suggested to have sub-lethal
301 behavioral effects on insects by blocking the mitochondrial electron transport chain. Inouye et al.
302 also showed the respiration-inhibitory effects of EOs on filamentous fungi (Inouye et al. 1998).
303 Similarly, modification of the mitochondria confirmed that fumigation with the *M. alternifolia* EO
304 affected the mitochondria in the thorax, where the mitochondria became enlarged and swollen.

305 This led to respiratory failure and energy deficiency in the insect body. The results were consistent
306 with those obtained in a previous study in which allyl isothiocyanate oil and PH_3 were used
307 (Mansour et al. 2012). Prates et al. (Prates et al. 1998) reported that terpenoids had lethal effects
308 on rice weevils because they affected the respiratory and digestive systems. The main components
309 of the *M. alternifolia* EO are terpinen-4-ol (40.09%), followed by γ-terpinene (21.85%), α-
310 terpinene (11.34%), α-terpineol (6.91%), and α-pinene (5.86%), which are all terpene compounds.
311 The findings of this study are also supported by the morphological alterations, represented by
312 matrix rarefaction and vacuolization, observed in the mitochondria.

313 However, insecticidal poisoning may occur by affecting different metabolic targets. A
314 previous study has reported that terpenes are very important components of EOs and prone to *in*
315 *vivo* metabolism by GST, CarE, and P450s in the insect body (Patra et al. 2015). Miyazawa et al.
316 (Miyazawa & Kumagae 2001) and Haigou et al. (Haigou & Miyazawa 2012) also showed that
317 terpinen-4-ol was prone to *in vivo* metabolism. In our study, the *T. confusum* transcriptome
318 revealed 54 transcripts that encode cytochrome P450s, with 18 differentially expressed more than
319 2-fold and 33 significantly increased ($p < 0.05$) under oil exposure (Table S3). These genes mainly
320 belong to the CYP6 family. This might explain why terpinen-4-ol can be metabolized by P450s
321 (Haigou & Miyazawa 2012). Most of the genes that encode CarEs and GSTs were also
322 significantly downregulated upon oil exposure (Table S3). The redundant components may bind
323 to the site of the enzyme, resulting in disturbance of the activity. When the conjugated xenobiotics
324 are translated into innocuous substances, the bound enzymes are damaged. This result is consistent
325 with that observed in a previous study. Overall, *T. confusum* probably uses these enzymes in

326 combination to catalyze and improve the transformation and degradation of exogenous
327 compounds, resulting in the enhancement of the immune system of the insect. Silencing the
328 upregulated gene expression may contribute to increasing the insecticidal activities of the EO.

329 Interestingly, we found that five transcripts encoding the subunits of NAD^+/NADH
330 dehydrogenase in complex I were significantly upregulated (Table S4). Our biochemical analysis
331 showed that the *M. alternifolia* EO caused pronounced inhibition of NADH but increased NAD^+
332 level from 12 to 60 h and then subsequently inhibited it. Complex I is the gatekeeper of the
333 respiratory chain and catalyzes the first step of NADH oxidation. NAD^+ is a biological oxidizing
334 agent in many metabolic reactions, and tNOX oxidizes hydroquinones and NADH, converting the
335 latter to the oxidized NAD^+ form (Titov et al. 2016). It elevates the NAD^+/NADH ratio and
336 translocates protons across the inner mitochondrial membrane, which ultimately leads to energy
337 production. To increase energy production in response to oil interference, *T. confusum* probably
338 coverts NADH excessively to the oxidized NAD^+, resulting in an increase in NAD^+ levels.
339 However, the regulatory mechanism of *T. confusum* is destroyed with time, resulting in a
340 significant reduction in NAD^+ levels. Therefore, *T. confusum* recovers the activity of NADH by
341 upregulating the expression of *NADH* genes; however, the NADH levels have been reduced
342 because of excessive conversion. This might explain our observation that the transcripts encoding
343 the subunits of NAD^+/NADH dehydrogenase were significantly upregulated at 24 h.

344 As reported by De et al., *Eugenia uniflora* L. (family, Myrtaceae) EO can inhibit the
345 respiratory electron transfer system established with an uncoupler (de Carvalho et al. 2017).
346 Parastoo et al. also found that *Tagetes minuta* EO significantly reduced NADH oxidase (Karimian

et al. 2014). Terpenes are the main constituents of the above-mentioned EOs and appears to play an important role in the cellular bioenergetic failure. Moreover, the *M. alternifolia* EO was observed to alter the morphology and ultrastructure of mitochondria in *Botrytis cinerea*, which causes mitochondrial dysfunction and disrupts the TCA cycle (Li et al. 2017). Thus, we concluded that NAD^+/NADH dehydrogenase may be the prime target for the *M. alternifolia* EO in insects, leading to blocking of the mitochondrial respiratory chain. This results in a dysfunctional energy system, damage to the mitochondria, and death.

CONCLUSIONS

To clarify the applicability of the findings of our previous study, we investigated the action of the *M. alternifolia* EO in degrading the mitochondria of *T. confusum*. Alterations to the mitochondria confirmed the insecticidal effect of the *M. alternifolia* EO, which may act by damaging the mitochondria. To better understand the insecticidal mechanism of the *M. alternifolia* EO, comparative transcriptome analysis of *T. confusum* using RNA-seq yielded a total of 2,208 DEGs in response to oil fumigation. The biochemical analysis showed that the intracellular NAD^+/NADH ratio is involved in the differential effect of the *M. alternifolia* EO. Thus, NAD^+/NADH dehydrogenase appears to be a prime target for pest control.

Supporting Information

Fig. S1. GO (a) and KEGG (b) pathway analysis of DEGs of *S. zeamais* after oil fumigation.

Table S1. qRT-PCR primers and primer efficiency.

Table S2. Top 22 enriched KEGG pathways between the oil-fumigated and control samples.

Table S3. Differentially expressed genes that encode respiration-related enzymes.

Table S4. Differentially expressed genes that encode xenobiotic detoxification-related enzymes.

REFERENCES

Abbott W. 1925. A method of computing the effectiveness of an insecticide. *J econ Entomol* 18:265-267.

Abdelgaleil SAM, Mohamed MIE, Shawir MS, and Abou-Taleb HK. 2015. Chemical composition, insecticidal and biochemical effects of essential oils of different plant species from Northern Egypt on the rice weevil, *Sitophilus oryzae* L. *Journal of Pest Science* 89:219-229. 10.1007/s10340-015-0665-z

Agarwala R, Barrett T, Beck J, Benson DA, Bollin C, Bolton E, Bourexis D, Brister JR, Bryant SH, Lanese K, Charowhas C, Clark K, DiCuccio M, Dondoshansky I, Federhen S, Feolo M, Funk K, Geer LY, Gorelenkov V, Hoeppner M, Holmes B, Johnson M, Khotomlianski V, Kimchi A, Kimelman M, Kitts P, Klimke W, Krasnov S, Kuznetsov A, Landrum MJ, Landsman D, Lee JM, Lipman DJ, Lu ZY, Madden TL, Madcj T, Marchler-Bauer A, Karsch-Mizrachi I, Murphy T, Orris R, Ostell J, O'Sullivan C, Panchenko A, Phan L, Preuss D, Pruitt KD, Rodarmer K, Rubinstein W, Sayers EW, Schneider V, Schuler GD, Sherry ST, Sirotkin K, Siyan K, Slotta D, Soboleva A, Soussov V, Starchenko G, Tatusova TA, Todorov K, Trawick BW, Vakatov D, Wang YL, Ward M, Wilbur WJ, Yaschenko E, Zbicz K, and Coordinators NR. 2016. Database resources of the National Center for Biotechnology Information. *Nucleic Acids Research* 44:D7-D19. 10.1093/nar/gkv1290

Ali-Shtayeh MS, Jamous RM, Abu-Zaitoun SY, Akkawi RJ, Kalbouneh SR, Dudai N, and Bernstein N. 2018. Secondary treated effluent irrigation did not impact chemical composition, and enzyme inhibition activities of essential oils from *Origanum syriacum* var. *syriacum*. *Industrial Crops and Products* 111:775-786.

Anders S, and Huber W. 2010. Differential expression analysis for sequence count data. *Genome Biology* 11. 10.1186/gb-2010-11-10-r106

Bai Y, Wang S, Zhong H, Yang Q, Zhang F, Zhuang Z, Yuan J, Nie X, and Wang S. 2015. Integrative analyses reveal transcriptome-proteome correlation in biological pathways and secondary metabolism clusters in *A. flavus* in response to temperature. *Sci Rep* 5:14582. 10.1038/srep14582

Bajda S, Dermauw W, Greenhalgh R, Nauen R, Tirry L, Clark RM, and Van Leeuwen T. 2015. Transcriptome profiling of a spirodiclofen susceptible and resistant strain of the European red mite *Panonychus ulmi* using strand-specific RNA-seq. *BMC genomics* 16.

Brahmi F, Abdenour A, Bruno M, Silvia P, Alessandra P, Danilo F, Drifa YG, Fahmi EM, Khodir M, and Mohamed C. 2016. Chemical composition and in vitro antimicrobial, insecticidal and antioxidant activities of the essential oils of *Mentha pulegium* L. and *Mentha rotundifolia* (L.) Huds growing in Algeria. *Industrial Crops and Products* 88:96-105.

Bustos-Segura C, Kulheim C, and Foley W. 2015. Effects of Terpene Chemotypes of *Melaleuca alternifolia* on Two Specialist Leaf Beetles and Susceptibility to Myrtle Rust. *Journal of Chemical Ecology* 41:937-947. 10.1007/s10886-015-0628-0

Chen Y, He M, Li ZQ, Zhang YN, and He P. 2016. Identification and tissue expression profile of genes from three chemoreceptor families in an urban pest, *Periplaneta americana*. *Sci Rep* 6. ARTN 2749510.1038/srep27495

Clements J, Schoville S, Peterson N, Lan Q, and Groves RL. 2016. Characterizing Molecular Mechanisms of Imidacloprid Resistance in Select Populations of Leptinotarsa decemlineata in the Central Sands Region of Wisconsin. *Plos One* 11:e0147844. 10.1371/journal.pone.0147844

Cock PJA, Fields CJ, Goto N, Heuer ML, and Rice PM. 2010. The Sanger FASTQ file format for sequences with quality scores, and the Solexa/Illumina FASTQ variants. *Nucleic Acids Research* 38:1767-1771.

Conesa A, Gotz S, Garcia-Gomez JM, Terol J, Talon M, and Robles M. 2005. Blast2GO: a universal tool for annotation, visualization and analysis in functional genomics research. *Bioinformatics* 21:3674-3676. 10.1093/bioinformatics/bti610

Correa AS, Tome HVV, Braga LS, Martins GF, de Oliveira LO, and Guedes RNC. 2014. Are mitochondrial lineages, mitochondrial lysis and respiration rate associated with phosphine susceptibility in the maize weevil Sitophilus zeamais? *Annals of Applied Biology* 165:137-146.

de Carvalho NR, Rodrigues NR, Macedo GE, Bristot IJ, Boligon AA, de Campos MM, Cunha FA, Coutinho HD, Klamt F, and Merritt TJ. 2017. Eugenia uniflora leaf essential oil promotes mitochondrial dysfunction in Drosophila melanogaster through the inhibition of oxidative phosphorylation. *Toxicology Research* 6:526-534.

Du SS, Yang K, Wang CF, You CX, Geng ZF, Guo SS, Deng ZW, and Liu ZL. 2014. Chemical constituents and activities of the essential oil from Myristica fragrans against cigarette beetle Lasioderma serricorne. *Chemistry & biodiversity* 11:1449-1456.

Du ZQ, Jin YH, and Ren DM. 2016. In-depth comparative transcriptome analysis of intestines of red swamp crayfish, *Procambarus clarkii*, infected with WSSV. *Sci Rep* 6. ARTN 26780
10.1038/srep26780

Enan E. 2001. Insecticidal activity of essential oils: octopaminergic sites of action. *Comparative Biochemistry and Physiology Part C: Toxicology & Pharmacology* 130:325-337.

Enan EE. 2005. Molecular response of Drosophila melanogaster tyramine receptor cascade to plant essential oils. *Insect Biochemistry and Molecular Biology* 35:309-321.

Fong DKH, Kim S, Chen Z, and DeSarbo WS. 2016. A Bayesian Multinomial Probit Model for the Analysis of Panel Choice Data. *Psychometrika* 81:161-183. 10.1007/s11336-014-9437-6

Golestan MN, Ghosta Y, Pourmirza AA, and Valizadegan O. 2015. Study on laser perforated films as gas permeable packaging for confused flour beetle (*Tribolium confusum Jacquelin* du Val.) control inside food packaging. *Journal of Stored Products Research* 60:54-59.

Grabherr MG, Haas BJ, Yassour M, Levin JZ, Thompson DA, Amit I, Adiconis X, Fan L, Raychowdhury R, Zeng QD, Chen ZH, Mauceli E, Hacohen N, Gnirke A, Rhind N, di Palma F, Birren BW, Nusbaum C, Lindblad-Toh K, Friedman N, and Regev A. 2011. Full-length transcriptome assembly from RNA-Seq data without a reference genome. *Nature Biotechnology* 29:644-U130.

Haddi K, Oliveira EE, Faroni LRA, Guedes DC, and Miranda NNS. 2015. Sublethal Exposure to Clove and Cinnamon Essential Oils Induces Hormetic-Like Responses and Disturbs Behavioral and Respiratory Responses in *Sitophilus zeamais* (Coleoptera: Curculionidae). *Journal of Economic Entomology* 108:2815-2822. 10.1093/jee/tov255

Haigou R, and Miyazawa M. 2012. Metabolism of (+)-Terpinen-4-ol by Cytochrome P450 Enzymes in Human Liver Microsomes. *Journal of oleo science* 61:35-43. 10.5650/jos.61.35

Hamisch D, Randewig D, Schliesky S, Brautigam A, Weber AP, Geffers R, Herschbach C, Rennenberg H, Mendel RR, and Hansch R. 2012. Impact of SO(2) on Arabidopsis thaliana transcriptome in wildtype and sulfite oxidase knockout plants analyzed by RNA deep sequencing. *New Phytologist* 196:1074-1085. 10.1111/j.1469-8137.2012.04331.x

448 Hao Y, Wang T, Wang K, Wang X, Fu Y, Huang L, and Kang Z. 2016. Transcriptome Analysis Provides Insights
449 into the Mechanisms Underlying Wheat Plant Resistance to Stripe Rust at the Adult Plant Stage. *Plos One*
450 11:e0150717. 10.1371/journal.pone.0150717
451 Hubert J, and Carter E. 1990. PROBIT: a program in PASCAL for univariate probit analysis with exact confidence
452 limits for LC50. *Statistical Series* 222.
453 Inouye S, Watanabe M, Nishiyama Y, Takeo K, Akao M, and Yamaguchi H. 1998. Antisporulating and
454 respiration-inhibitory effects of essential oils on filamentous fungi. *Mycoses* 41:403-410.
455 Kanehisa M, and Goto S. 2000. KEGG: Kyoto Encyclopedia of Genes and Genomes. *Nucleic Acids Research* 28:27-
456 30. DOI 10.1093/nar/28.1.27
457 Karimian P, Kavoosi G, and Amirghofran Z. 2014. Anti–oxidative and anti–inflammatory effects of Tagetes minuta
458 essential oil in activated macrophages. *Asian Pacific Journal of Tropical Biomedicine* 4:219-227.
459 https://doi.org/10.1016/S2221-1691(14)60235-5
460 Kim D, Pertea G, Trapnell C, Pimentel H, Kelley R, and Salzberg SL. 2013a. TopHat2: accurate alignment of
461 transcriptomes in the presence of insertions, deletions and gene fusions. *Genome Biology* 14.
462 Kim SW, Kang J, and Park IK. 2013b. Fumigant toxicity of Apiaceae essential oils and their constituents against
463 *Sitophilus oryzae* and their acetylcholinesterase inhibitory activity. *Journal of Asia-Pacific Entomology*
464 16:443-448. 10.1016/j.aspen.2013.07.002
465 Kiran S, Kujur A, Patel L, Ramalakshmi K, and Prakash B. 2017. Assessment of toxicity and biochemical mechanisms
466 underlying the insecticidal activity of chemically characterized *Boswellia carterii* essential oil against insect
467 pest of legume seeds. *Pesticide Biochemistry and Physiology* 139:17-23.
468 Langmead B, Trapnell C, Pop M, and Salzberg SL. 2009. Ultrafast and memory-efficient alignment of short DNA
469 sequences to the human genome. *Genome Biology* 10.
470 Li B, and Dewey CN. 2011. RSEM: accurate transcript quantification from RNA-Seq data with or without a reference
471 genome. *BMC bioinformatics* 12.
472 Li S-G, Li M-Y, Huang Y-Z, Hua R-M, Lin H-F, He Y-J, Wei L-L, and Liu Z-Q. 2013. Fumigant activity of *Illicium*
473 *verum* fruit extracts and their effects on the acetylcholinesterase and glutathione S-transferase activities in
474 adult Sitophilus zeamais. *Journal of Pest Science* 86:677-683. 10.1007/s10340-013-0520-z
475 Li Y, Shao X, Xu J, Wei Y, Xu F, and Wang H. 2017. Tea tree oil exhibits antifungal activity against Botrytis cinerea
476 by affecting mitochondria. *Food Chemistry* 234:62-67. https://doi.org/10.1016/j.foodchem.2017.04.172
477 Liang J-y, Wang W-t, Zheng Y-f, Zhang D, Wang J-l, Guo S-s, Zhang W-j, Du S-s, and Zhang J. 2017. Bioactivities
478 and chemical constituents of essential oil extracted from *Artemisia anethoides* against two stored product
479 insects. *Journal of oleo science* 66:71-76.
480 Liang J-y, You C-x, Guo S-s, Zhang W-j, Li Y, Geng Z-f, Wang C-f, Du S-s, Deng Z-w, and Zhang J. 2016. Chemical
481 constituents of the essential oil extracted from *Rhododendron thymifolium* and their insecticidal activities
482 against Liposcelis bostrychophila or Tribolium castaneum. *Industrial Crops and Products* 79:267-273.
483 Liao M, Xiao JJ, Zhou LJ, Liu Y, Wu XW, Hua RM, Wang GR, and Cao HQ. 2016. Insecticidal Activity of *Melaleuca*
484 *alternifolia* Essential Oil and RNA-Seq Analysis of Sitophilus zeamais Transcriptome in Response to Oil
485 Fumigation. *Plos One* 11. ARTN e016774810.1371/journal.pone.0167748
486 Ma Z, Tan Y, Cui G, Feng Y, Cui Q, and Song X. 2015. Transcriptome and gene expression analysis of DHA producer
487 Aurantiochytrium under low temperature conditions. *Sci Rep* 5:14446. 10.1038/srep14446
488 Mansour EE, Mi F, Zhang G, Jiugao X, Wang Y, and Kargbo A. 2012. Effect of allylisothiocyanate on *Sitophilus*

oryzae, *Tribolium confusum* and *Plodia interpunctella*: Toxicity and effect on insect mitochondria. *Crop Protection* 33:40-51.

Miyazawa M, and Kumagae S. 2001. Biotransformation of (R)- and (S)-terpinen-4-ol by the Larvae of Common Cutworm (*Spodoptera litura*). *Journal of Agricultural and Food Chemistry* 49:4312-4314. DOI 10.1021/jf010273t

Oter ALC, Palacio-Cortes AM, Navarro-Silva MA, Kouznetsov VV, and Duque JE. 2018. Behavior of detoxifying enzymes of Aedes aegypti exposed to girgensohnine alkaloid analog and Cymbopogon flexuosus essential oil. *Comparative Biochemistry and Physiology C-Toxicology & Pharmacology* 204:14-25. 10.1016/j.cbpc.2017.11.002

Pan HP, Yang XW, Siegfried BD, and Zhou XG. 2015. A Comprehensive Selection of Reference Genes for RT-qPCR Analysis in a Predatory Lady Beetle, *Hippodamia convergens* (Coleoptera: Coccinellidae). *Plos One* 10. UNSP e012586810.1371/journal.pone.0125868

Patra JK, Das G, and Baek KH. 2015. Antibacterial mechanism of the action of *Enteromorpha linza L*. essential oil against *Escherichia coli* and *Salmonella Typhimurium*. *Botanical Studies* 56. ARTN 1310.1186/s40529-015-0093-7

Polatoglu K, Karakoc OC, Yucel YY, Gucel S, Demirci B, Baser KHC, and Demirci F. 2016. Insecticidal activity of edible *Crithmum maritimum L*. essential oil against Coleopteran and Lepidopteran insects. *Industrial Crops and Products* 89:383-389.

Prates HT, Santos JP, Waquil J, Fabris J, and De Oliveira A. 1998. *The potential use of plant substances extracted from Brazilian flora to control stored grain pest*.

Schmittgen TD, and Livak KJ. 2008. Analyzing real-time PCR data by the comparative C-T method. *Nature protocols* 3:1101-1108. 10.1038/nprot.2008.73

Silva SM, Haddi K, Jumbo LOV, and Oliveira EE. 2017. Progeny of the maize weevil, *Sitophilus zeamais*, is affected by parental exposure to clove and cinnamon essential oils. *Entomologia Experimentalis Et Applicata* 163:220-228. 10.1111/eea.12559

Stone JD, and Storchova H. 2015. The application of RNA-seq to the comprehensive analysis of plant mitochondrial transcriptomes. *Molecular Genetics and Genomics* 290:1-9. 10.1007/s00438-014-0905-6

Tatusov RL, Galperin MY, Natale DA, and Koonin EV. 2000. The COG database: a tool for genome-scale analysis of protein functions and evolution. *Nucleic Acids Research* 28:33-36. DOI 10.1093/nar/28.1.33

Titov DV, Cracan V, Goodman RP, Peng J, Grabarek Z, and Mootha VK. 2016. Complementation of mitochondrial electron transport chain by manipulation of the NAD(+)/NADH ratio. *Science* 352:231-235.

Vanhaelen N, Haubruge E, and Francis F. 2001. Effects of Brassicaceae secondary metabolites on the Glutathione S-transferase activity from *Episyrphus balteatus* De Geer (Diptera: Syrphidae). *Pesticide Biochemistry & Physiology* 71:170-177.

Wu Y, Zhang WJ, Huang DY, Wang Y, Wei JY, Li ZH, Sun JS, Bai JF, Tian ZF, Wang PJ, and Du SS. 2015. Chemical Compositions and Insecticidal Activities of *Alpinia kwangsiensis* Essential Oil against *Lasioderma serricorne*. *Molecules* 20:21939-21945. 10.3390/molecules201219818

Xu M, Xu FY, and Wu XQ. 2017. Differentially Expressed Proteins From the Peritrophic Membrane Related to the Lethal, Synergistic Mechanisms Observed in *Hyphantria cunea* Larvae Treated With a Mixture of Bt and Chlorbenzuron. *Journal of Insect Science* 17.

Yeom HJ, Kang J, Kim SW, and Park IK. 2013. Fumigant and contact toxicity of *Myrtaceae* plant essential oils and

530 blends of their constituents against adults of German cockroach (*Blattella germanica*) and their
531 acetylcholinesterase inhibitory activity. *Pesticide Biochemistry and Physiology* 107:200-206.

Table 1(on next page)

Summary of the sequencing reads of the *T. confusum* transcriptome and corresponding assemblies and statistics of the annotation results.

Table legends

Table 1. Summary of the sequencing reads of the *T. confusum* transcriptome and corresponding assemblies and statistics of the annotation results.

		Control	Treatment
Raw reads	Total number	64,760,250	61,519,782
Clean reads	Total number	45,114,010	44,228,536
	Total nucleotides (nt)	4,511,401,000	4,422,853,600
	Q20 (%)	97.38	97.55
Contigs	Total number	34,747	33,988
	Mean length (bp)	1,043	1,042
Primary unigenes	Total number	26,367	25,883
Final unigenes	Total number	28,885	
	Total length (bp)	36,998,010	
	Mean length (bp)	1,280	
	N50 (bp)	2,097	
	GC (%)	37.39	
	Number, < 600 bp	38.54	
	Number, ≥ 600 bp	61.46	
Annotation	Nr	23,160 (80.18%)	
	Nt	9,941 (34.42%)	
	COG	9,451 (32.72%)	
	KEGG	18,074 (62.57%)	
	GO	6,333 (21.92%)	
	Swiss-Prot	18,187 (62.96%)	
	InterPro	17,837 (61.75%)	
	All databases	23,571 (81.60%)	

Figure 1

Fumiganttoxicity of *M. alternifolia* essential oil (a) and its constituents (c)against *T. confusum* adults and the corresponding regression analysis(b).

Results are reported as mean ± SE (calculated from three independent experiments). The LC_{50} values were subjected to probit analysis. (Fong et al. 2016) Different lowercase letters at the top of the columns mean significant differences at a *p* value of 0.05. The error in Figure 3c represents the 95% fiducial limits.

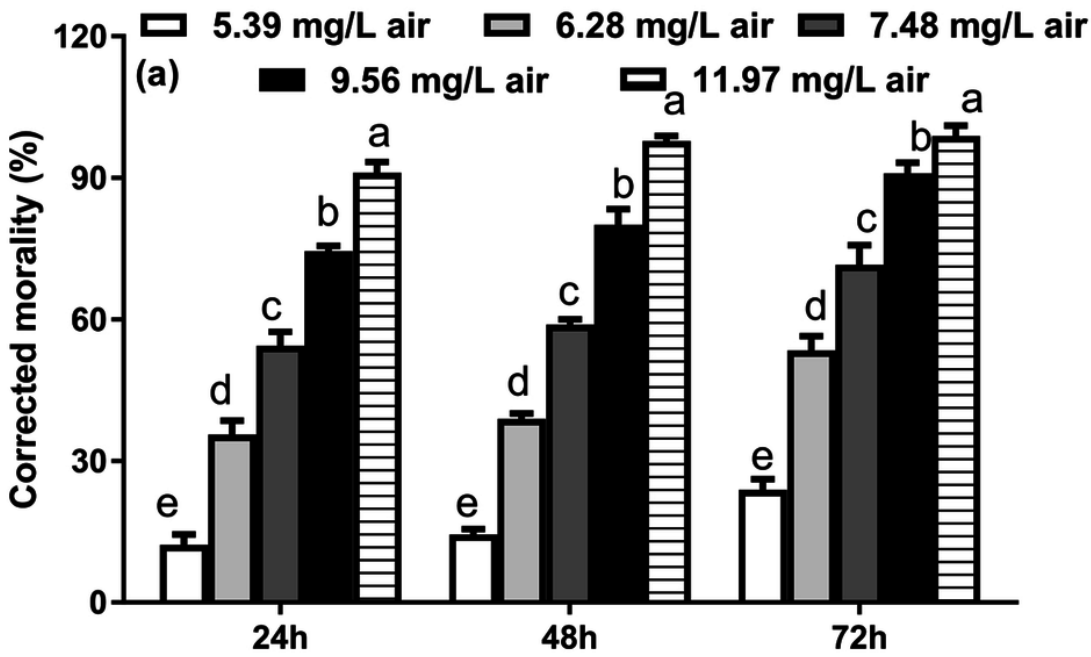
5.39 mg/L air
6.28 mg/L air
7.48 mg/L air
9.56 mg/L air
11.97 mg/L air
(a)
Corrected morality (%)
120
90
60
30
0
24h
48h
72h

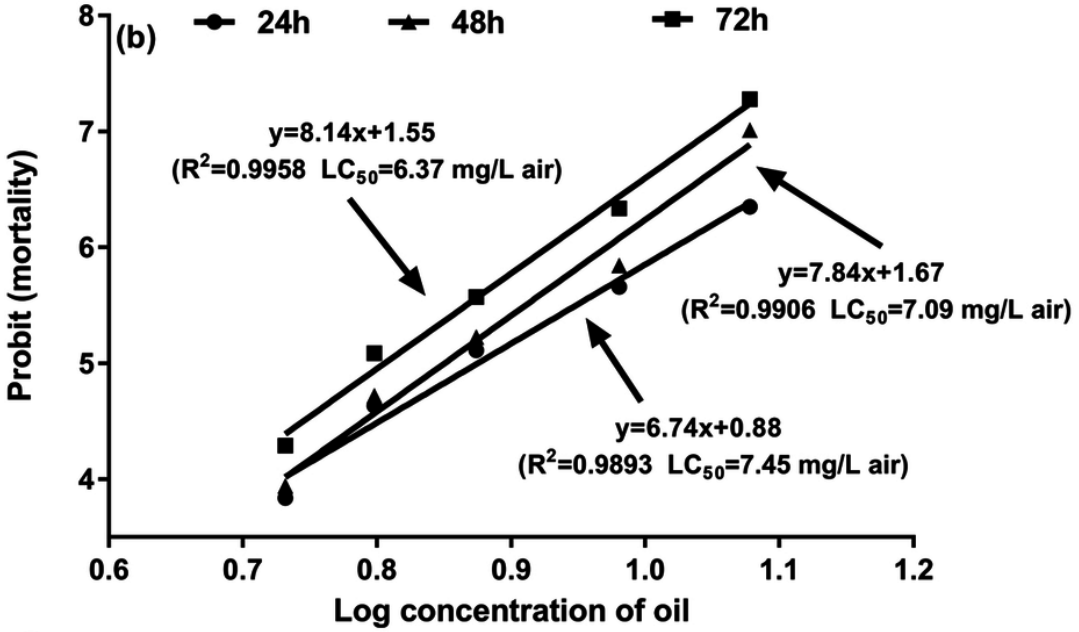
(b)
24h
48h
72h
Probit (mortality)
y=8.14x+1.55
(R²=0.9958 LC50=6.37 mg/L air)
y=7.84x+1.67
(R²=0.9906 LC50=7.09 mg/L air)
y=6.74x+0.88
(R²=0.9893 LC50=7.45 mg/L air)
Log concentration of oil

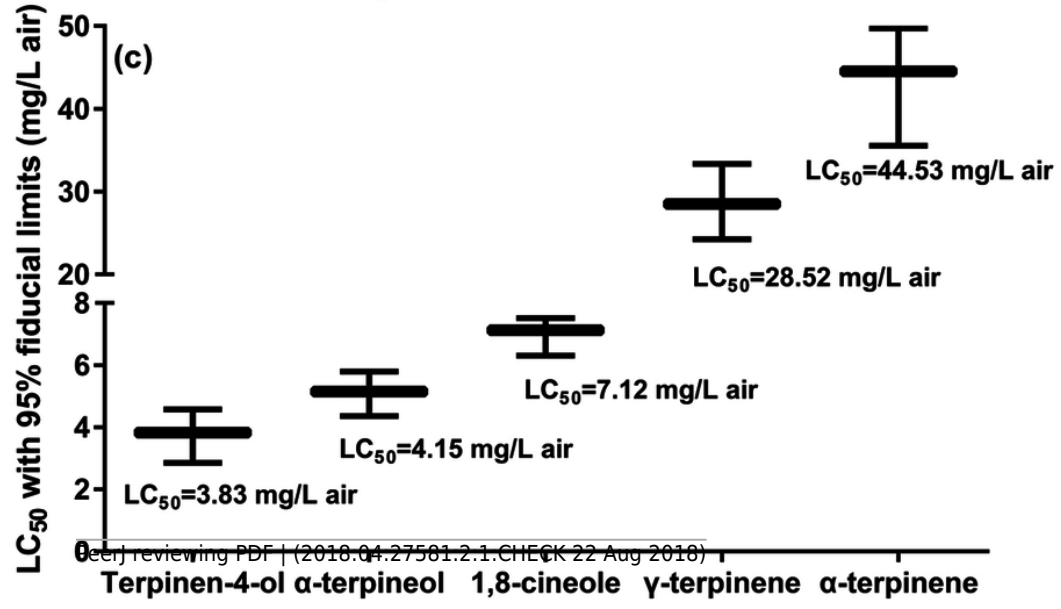
(c)
LC50 with 95% fiducial limits (mg/L air)
LC50=44.53 mg/L air
LC50=28.52 mg/L air
LC50=7.12 mg/L air
LC50=4.15 mg/L air
LC50=3.83 mg/L air
Terpinen-4-ol
α-terpineol
1,8-cineole
γ-terpinene
α-terpinene

Figure 2

Ultra-structure of the mitochondria from the thorax of non-fumigated (a, c, and e) and fumigated (b, d, and f) *T. confusum* adults.

A: The normal structure of the mitochondrion with many highly electron-dense cristae. B: A part of the thorax and ultra-structural changes in the mitochondria represented by vacuolization (Vm) and rarefaction (Rm) of the mitochondrial matrix (arrow). C: The vacuolization aggravated 24 (b), 48 (d), and 72 h (f) after oil treatment. Scale bar = 2.0 μm.

**Note: Auto Gamma Correction was used for the image. This only affects the reviewing manuscript. See original source image if needed for review.*

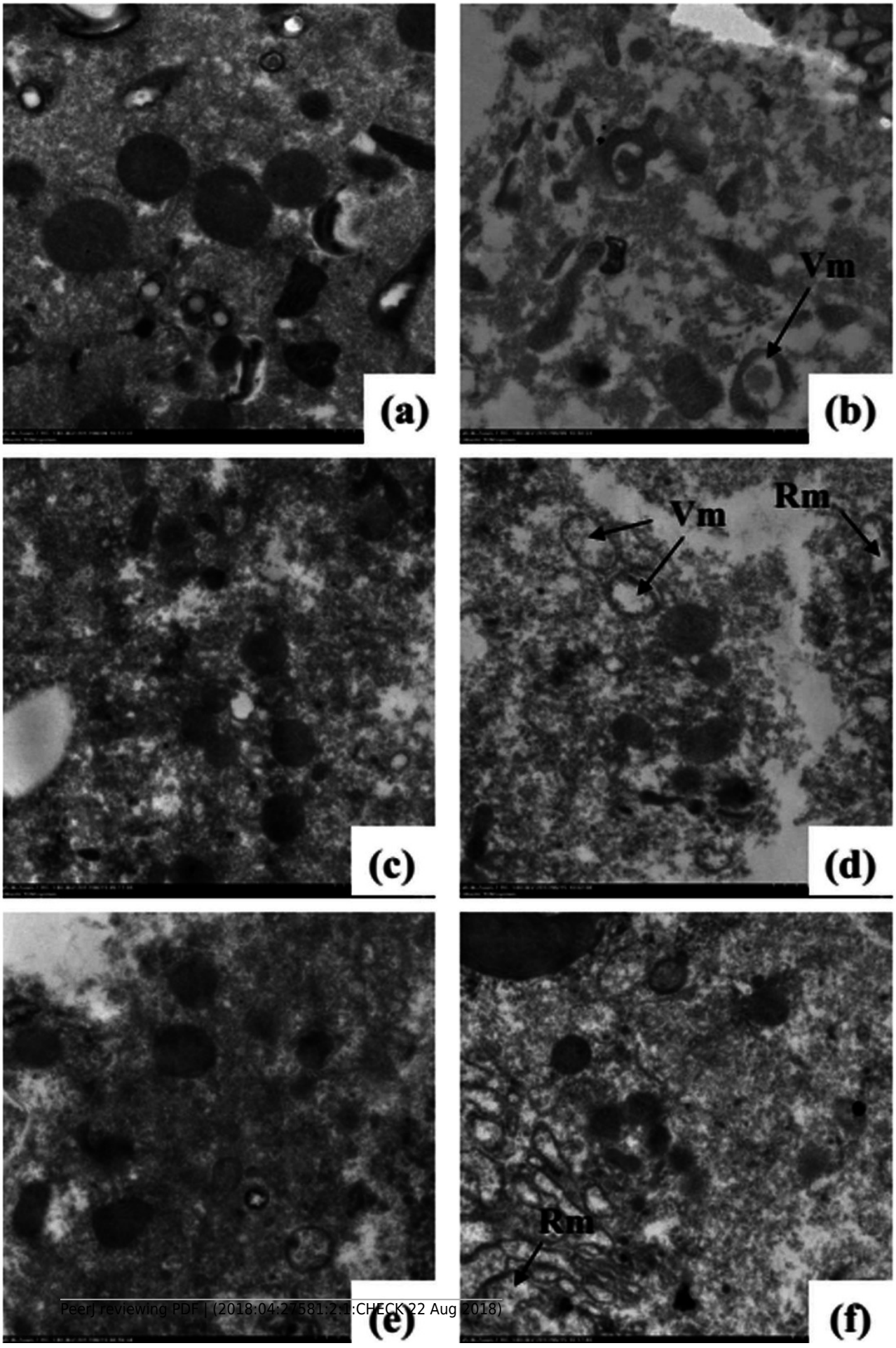
(a)
Vm
(b)
(c)
Vm
Rm
(d)
Rm
(f)

Figure 3

Length distribution of assembled sequences (a) and GO (b) and KEGG (c) functional classifications of assembled unigenes of *T. confusum*.

The reads from four libraries were assembled into 2,8885 transcripts.

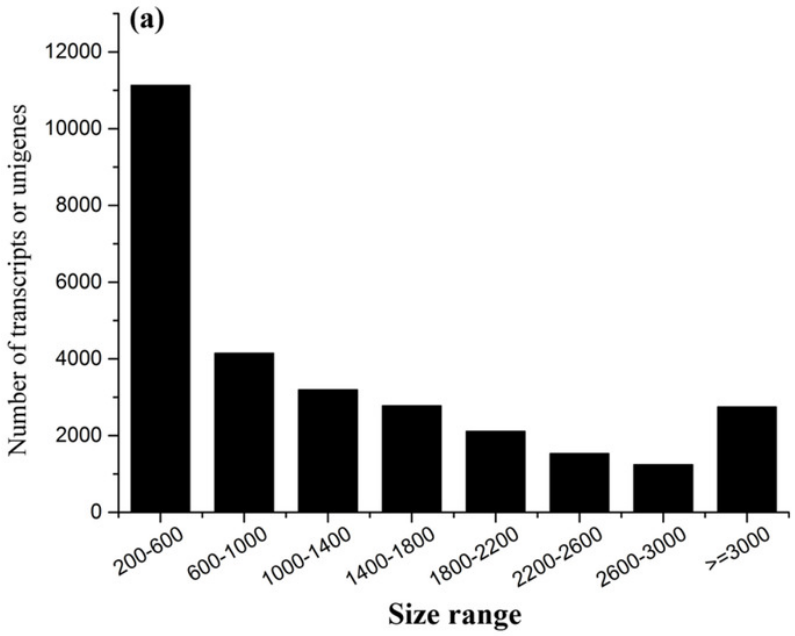
(a)
Number of transcripts or unigenes
0
2000
4000
6000
8000
10000
12000
200-600
600-1000
1000-1400
1400-1800
1800-2200
2200-2600
2600-3000
>=3000
Size range

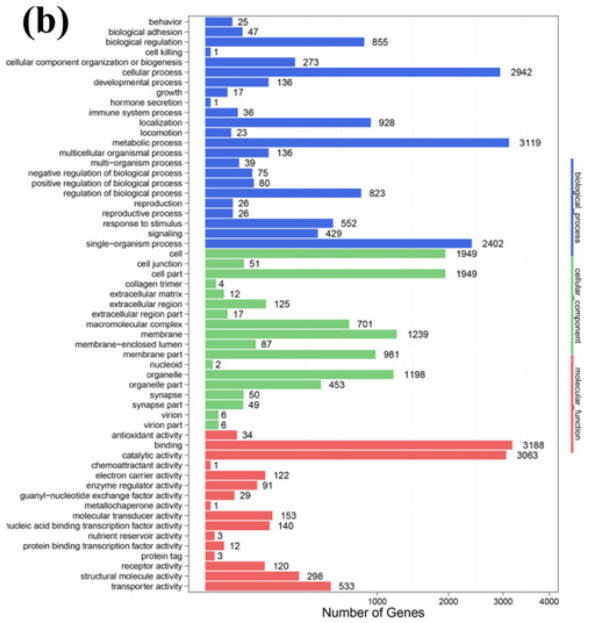
(b)
behavior 25
biological adhesion 47
biological regulation 855
cell killing 1
cellular component organization or biogenesis 273
cellular process 2942
developmental process 136
growth 17
hormone secretion 1
immune system process 36
localization 928
locomotion 23
metabolic process 3119
multicellular organismal process 136
multi-organism process 39
negative regulation of biological process 75
positive regulation of biological process 80
regulation of biological process 823
reproduction 26
reproductive process 26
response to stimulus 552
signaling 429
single-organism process 2402
cell 1949
cell junction 51
cell part 1949
collagen trimer 4
extracellular matrix 12
extracellular region 125
extracellular region part 17
macromolecular complex 701
membrane 1239
membrane-enclosed lumen 87
membrane part 981
nucleoid 2
organelle 1198
organelle part 453
synapse 50
synapse part 49
virion 6
virion part 6
antioxidant activity 34
binding 3188
catalytic activity 3063
chemoattractant activity 1
electron carrier activity 122
enzyme regulator activity 91
guanyl-nucleotide exchange factor activity 29
metallochaperone activity 1
molecular transducer activity 153
nucleic acid binding transcription factor activity 140
nutrient reservoir activity 3
protein binding transcription factor activity 12
protein tag 3
receptor activity 120
structural molecule activity 298
transporter activity 533
biological process
cellular component
molecular function
1000
2000
3000
4000
Number of Genes

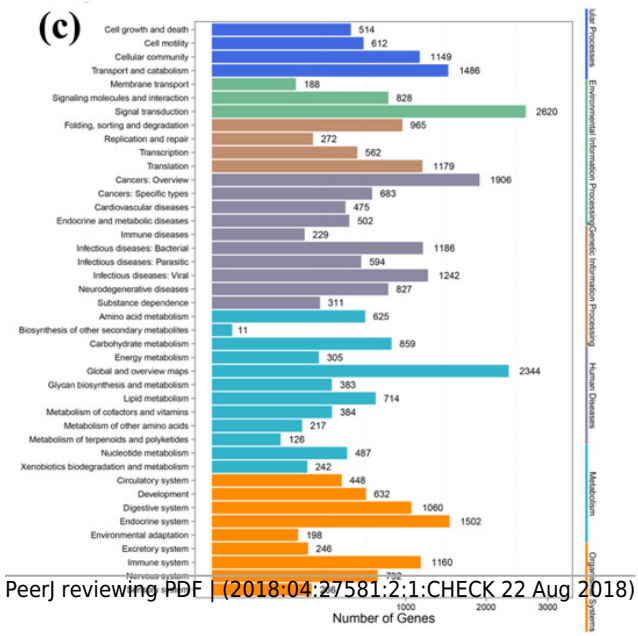
(c)
Cell growth and death 514
Cell motility 612
Cellular community 1149
Transport and catabolism 1486
Membrane transport 188
Signaling molecules and interaction 828
Signal transduction 2620
Folding, sorting and degradation 965
Replication and repair 272
Transcription 562
Translation 1179
Cancers: Overview 1906
Cancers: Specific types 683
Cardiovascular diseases 475
Endocrine and metabolic diseases 502
Immune diseases 229
Infectious diseases: Bacterial 1186
Infectious diseases: Parasitic 594
Infectious diseases: Viral 1242
Neurodegenerative diseases 827
Substance dependence 311
Amino acid metabolism 625
Biosynthesis of other secondary metabolites 11
Carbohydrate metabolism 859
Energy metabolism 305
Global and overview maps 2344
Glycan biosynthesis and metabolism 383
Lipid metabolism 714
Metabolism of cofactors and vitamins 384
Metabolism of other amino acids 217
Metabolism of terpenoids and polyketides 126
Nucleotide metabolism 487
Xenobiotics biodegradation and metabolism 242
Circulatory system 448
Development 632
Digestive system 1060
Endocrine system 1502
Environmental adaptation 198
Excretory system 246
Immune system 1160
Nervous system 732
Cellular Processes
Environmental Information Processing
Genetic Information Processing
Human Diseases
Metabolism
Organismal Systems
1000
2000
3000
Number of Genes

Figure 4

Real-time qRT-PCR analysis of DEGs that encode respiration and detoxification-related enzymes in *T. confusum* after oil fumigation.

Gene expression (mean ± SE) was quantified as relative fold change by using the $2^{-\Delta\Delta CT}$ method. The asterisks indicate significant differences in the expression level of DEGs between the oil-treated and no-oil-treated samples (* p value < 0.05 and ** p value < 0.01).

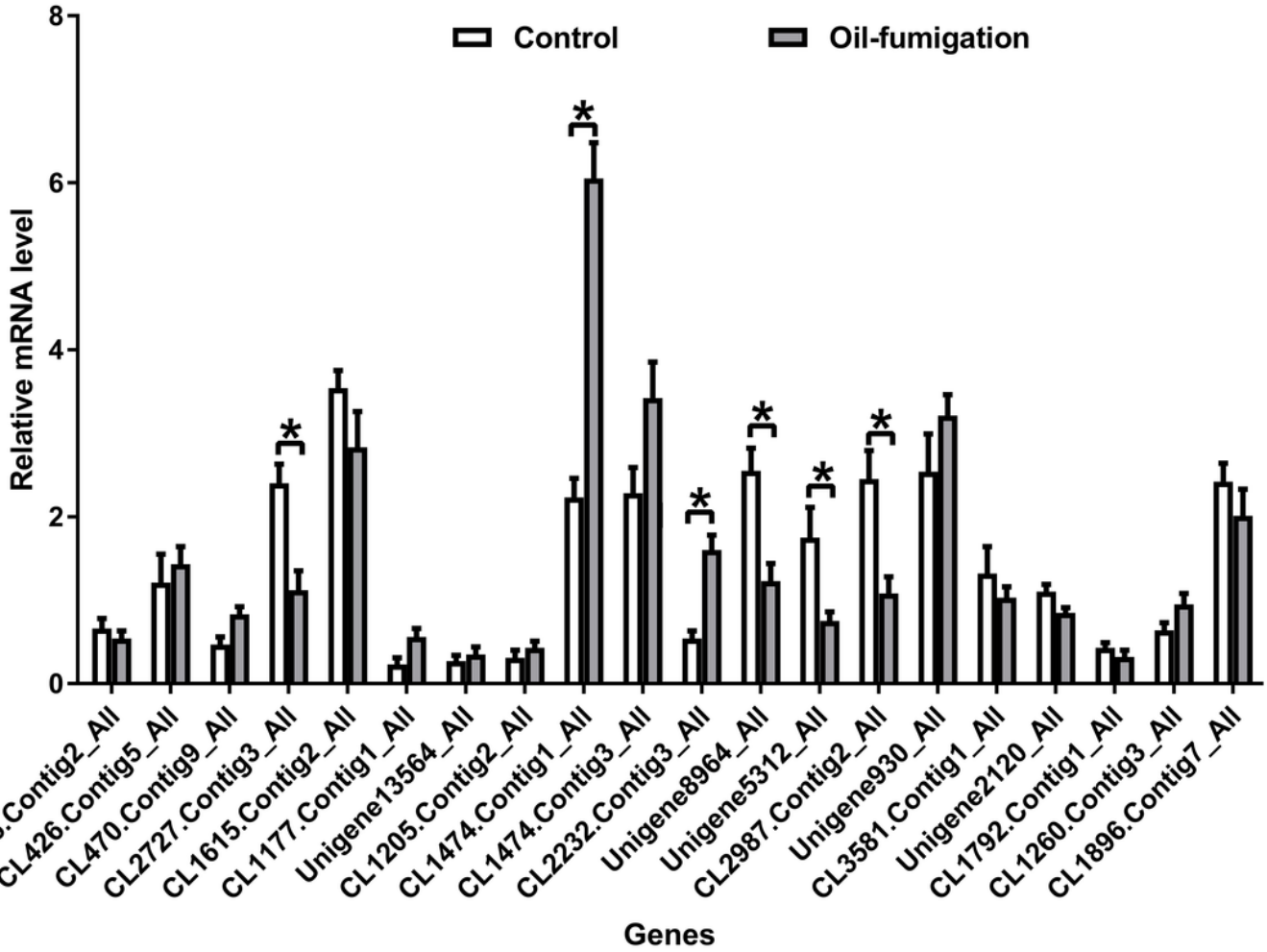

Figure 5

NAD^+ (a) and NADH (b) in the control and oil-fumigated *T. confusum* extracts were quantified.

Optical density at 450 nm was recorded and used to calculate the NADH/NAD^+ ratio (c). Values (mean ± SE) are from three independent experiments: ($*$) $p < 0.05$ and ($**$) $p < 0.001$ for oil fumigation (LC_{50} = 6.37 mg/L air) versus control (CK).

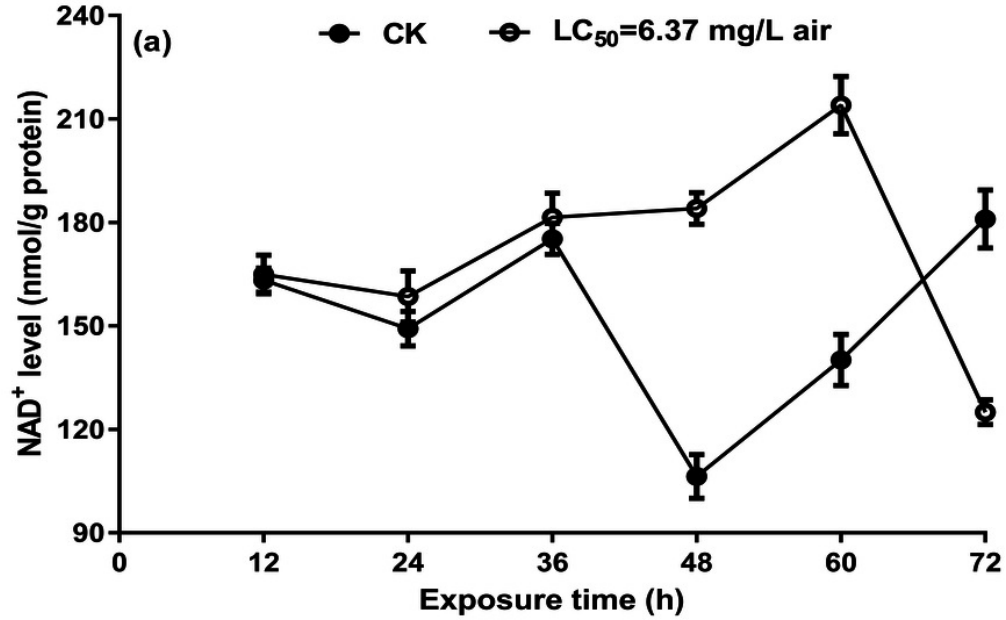
(a)
CK
LC50=6.37 mg/L air
NAD+ level (nmol/g protein)
240
210
180
150
120
90
0
12
24
36
48
60
72
Exposure time (h)

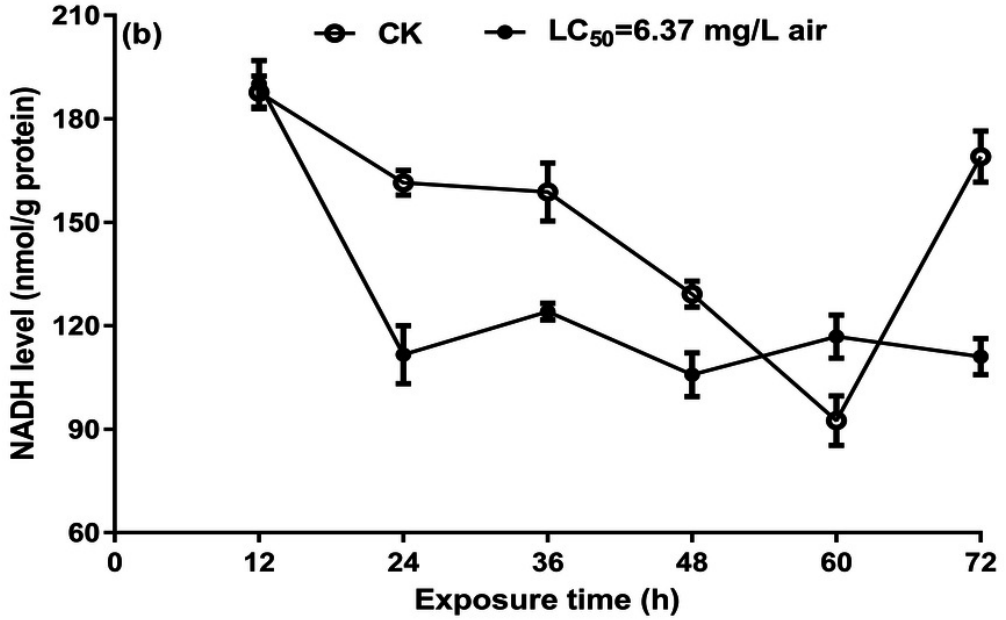
(b)
CK
LC50=6.37 mg/L air
NADH level (nmol/g protein)
210
180
150
120
90
60
0
12
24
36
48
60
72
Exposure time (h)

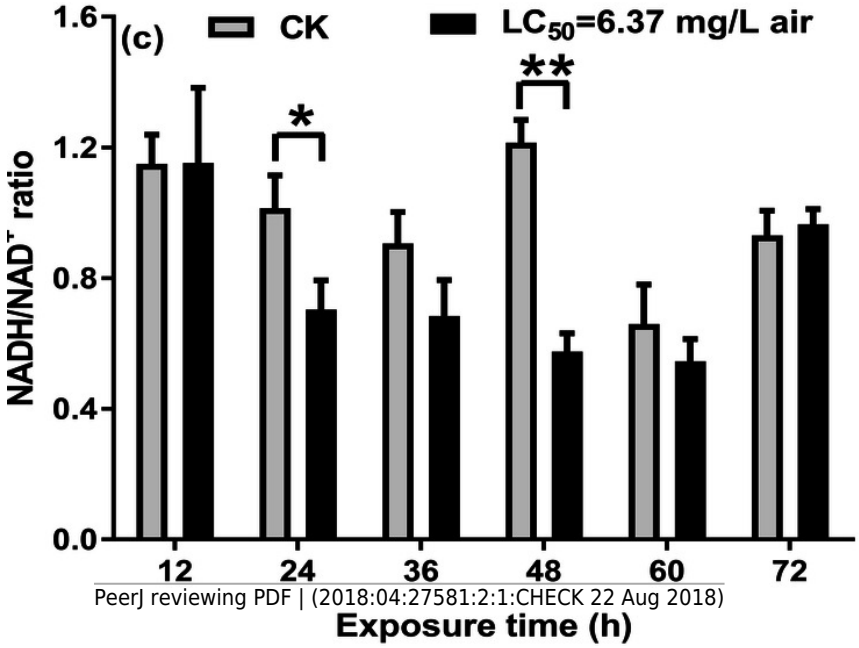
(c)
CK
LC50=6.37 mg/L air
*
**
NADH/NAD+ ratio
1.6
1.2
0.8
0.4
0.0
12
24
36
48
60
72
Exposure time (h)